Int J Appl Earth Obs Geoinformation 93 (2020) 102211

Contents lists available at ScienceDirect

Int J Appl Earth Obs Geoinformation

journal homepage: www.elsevier.com/locate/jag

Assessing Worldview-3 multispectral imaging abilities to map the tree diversity in semi-arid parklands

Camille C.D. Lelong[a,b,*,1], Urcel Kalenga Tshingomba[a,b,c,d,1], Valérie Soti[c,d,1]

[a] CIRAD, UMR TETIS, F-34398 Montpellier, France
[b] TETIS, Univ Montpellier, CIRAD, Montpellier, France
[c] CIRAD, UR AIDA, F-34398 Montpellier, France
[d] AIDA, Univ Montpellier, CIRAD, Montpellier, France

ARTICLE INFO

Keywords:
Worldview-3
Very high resolution
Classification
Support vector machine
Random forest
Tree mapping
Species discrimination
Agroforestry
Parkland
Ecosystem services

ABSTRACT

Semi-arid parkland agrosystems are strongly sensitive to climate change and anthropic pressure. In the context of sustainability research, trees are considered critical for various ecosystem services covering environment quality as well as food security and health. But their actual ecological impact on both cropland and natural vegetation is not well understood yet, and collecting spatial and structural information around agroforestry systems is becoming an important issue. Tree mapping in semi-arid parklands could be one of these prerequisites. While for obtaining an exhaustive inventory of individual trees and for analysing their spatial distribution, remote sensing is the ideal tool. However, it has been noted that depending on the spatial resolution and sensor spectral characteristics, tree species cannot be distinguished clearly, even in the sparsely vegetated semi-arid ecosystems of West Africa. Thus, this work focuses on assessing the capabilities of Worldview-3 imagery, acquired in 8 spectral bands, to detect, delineate, and identify certain key tree species in the *Faidherbia albida* parkland in Bambey, Senegal, based on a ground-truth database corresponding to 5000 trees. The tree crowns are delineated through NDVI thresholding and consecutive filtering to provide object-based radiometric signatures, radiometric indices, and textural information. A factorial discriminant analysis is then performed, which indicates that only four out of the seven most abundant species in the study area can be discriminated: "*Faidherbia albida*"," *Azadirachta indica*", "*Balanites aegyptiaca*" and "*Tamarindus indica*". Next, random forest and support vector machine classifiers are employed to identify the optimal combination of classifier parameters to discriminate these classes with a high accuracy, robustness, and stability. The linear support vector machine with cost = 1 and gamma = 0.01 provides the optimal results with a global accuracy of 88 % and kappa of 0.71. This classifier is applied to the whole study area to map all the trees with crowns larger than 2 m, sorted in four identified species and a fifth common group of unidentified species. This map thus enables analysing the variability in tree density and the spatial distribution of different species. Such information can afterwards be correlated to the ecological functioning of the parkland and local practices, and offers promising opportunities to help future sustainability initiatives in different socio-ecological contexts.

1. Introduction

Trees are key information for studying agroforestry ecosystems (Nagendra et al., 2004; Wulder et al., 2004), and understanding their spatial distribution is crucial when assessing the conservation status of tree populations and predicting responses to environmental and climatic changes (Cabello and Fernández, 2012). In various ways, trees are beneficial to their environment by, for example, improving air quality, preserving soil, and supporting wildlife. In agroforestry, the properties of parkland trees to improve soil fertility (Ajayi and Place, 2011; Akinnifesi and Ajayi, 2010) and to retain water (Sileshi et al., 2011; Verchot and Noordwijk, 2007), are widely used to enhance surrounding crop yields (Garrity, 2004; Syampungani et al., 2010). A denser tree cover inside or around agricultural fields could prevent soil erosion and protect from wind damage (Alemu, 2016). Increased tree cover often, but not always, reduces pest pressures and improves pollination services (Gurr et al., 2003; Bianchi et al., 2006; Dix et al., 1995; Zhang et al., 2007; Pumariño et al., 2015; Tscharntke et al., 2016).

* Corresponding author.
E-mail addresses: camille.lelong@cirad.fr (C.C.D. Lelong), valerie.soti@cirad.fr (V. Soti).
[1] As equal authors.

https://doi.org/10.1016/j.jag.2020.102211
Received 30 April 2020; Received in revised form 25 June 2020; Accepted 30 July 2020
Available online 05 August 2020

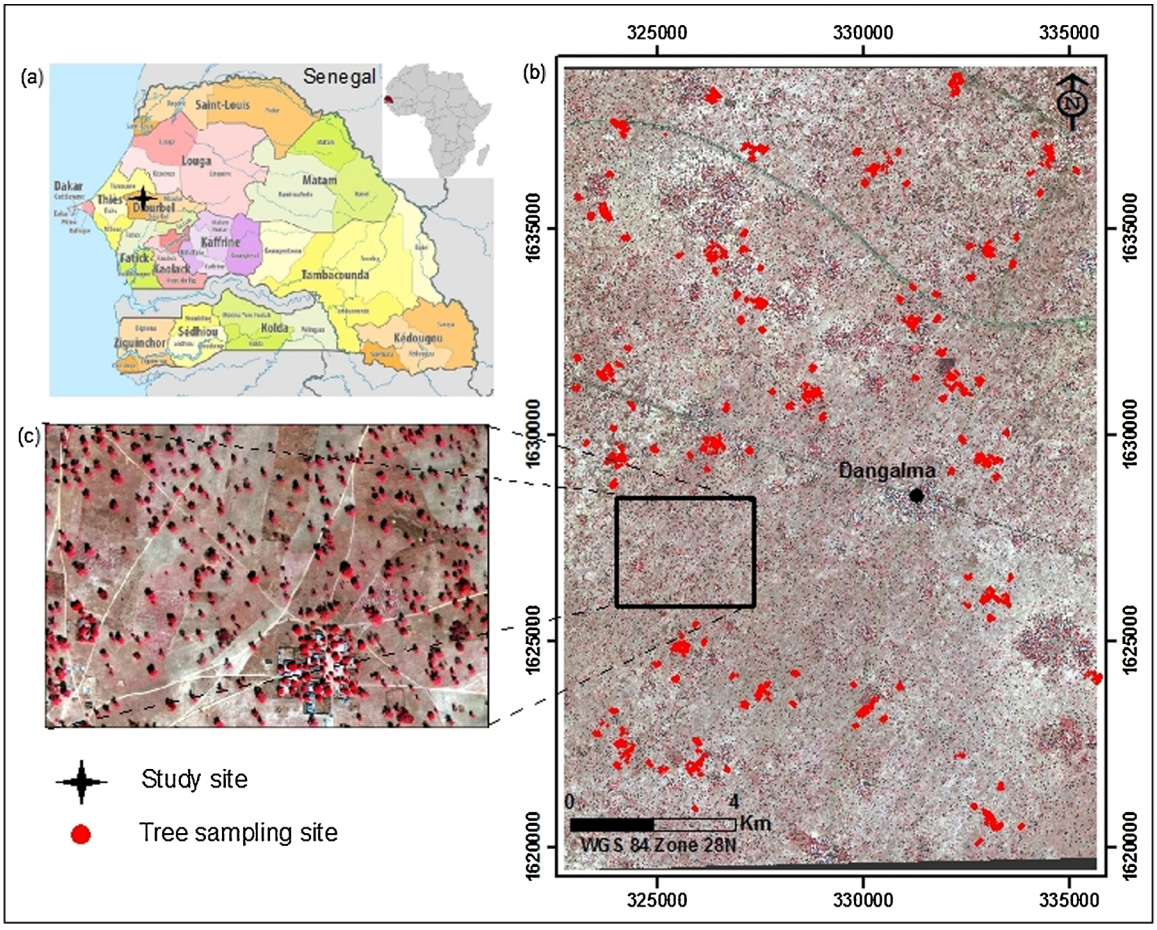

Fig. 1. (a) Location of the study area; (b) WV-3 image of the study area and location of the sampled trees in the field; (c) Zoomed in view of the WV-3 image in the pansharpened mode (0.30 m/pixel).

Moreover, trees and their diversity play an important role for the local economy (Pélissier, 1980; Depommier 1996) providing to rural population a source of fuelwood, medicinal plants, food, and fodder-scarce commodities in many arid and semi-arid regions. Unfortunately, the accelerated destruction of tree species around the world is ongoing, threatening the associated ecosystem services (ESs) and plant and animal biodiversity (World Health Organization., 2005). In the face of this fragmentation of natural areas, agroforestry appears to be a promising alternative for the sustainable management of cultivated areas. Indeed, the multifunctional role of agroforestry, that can simultaneously support income, food security, ESs and biodiversity conservation (Tscharntke and Clough, 2012; Kuyah et al., 2016), is broadly considered as critical for decision making in the search for sustainability (Reid et al., 2005; Carpenter et al., 2009).

The development of international initiatives, such as the Millennium Ecosystem Assessment (Reid et al., 2005), emphasizes the need to collect information around ESs for balancing human well-being with the maintenance of crucial ecological processes (Perrings et al., 2011). Therefore, timely and detailed information acquisition on the spatial distribution and structural characteristics of trees within agroforestry systems is critical for better understanding their eco-service values, and subsequently for developing sustainable forest and agriculture management strategies (Lindenmayer et al., 2000). Traditional field-based inventories are not suitable over large geographic areas, and enhanced methods are thus required to obtain spatially explicit information on the composition and distribution patterns of the tree species (Turner and Spector, 2003). In this regard, the use of remote sensing data is being widely explored for biodiversity monitoring and conservation (Alleaume and Dusseux, 2018; Lausch and Bannehr, 2016; Pettorelli and Bühne, 2018; Rocchini and Boyd, 2016; Vihervaara and Auvinen, 2017) due to its extensive spatial coverage and revisit capacity (McDermid and Hall, 2009; Nagendra, 2001; Wulder et al., 2004). Until recently, the remote sensing identification of tree species has been mainly performed using data from airborne hyperspectral sensors and LIDAR imagery (Cho and Debba, 2010; Clark et al., 2005; Dalponte et al., 2012; Féret and Asner, 2011; Naidoo et al., 2012; Verlič and Đurić, 2014). However, the high cost and difficulty of performing flight campaigns limit the application of such approaches. The latest generations of very high spatial resolution sensors allow the realisation of deeper analyses at finer levels of detail, with image footprints of approximately 400 km^2 and sub-metric spatial resolutions. The development of such sensors and methods may give effective and inexpensive alternatives for numerous new applications including tree species inventory and mapping at the crown scale, which is the key topic of interest of this study. Recently, promising results for tree species identification in temperate forest ecosystems (Immitzer et al., 2012; Waser et al., 2014), urban forests (Verlič and Đurić, 2014), mangroves (Heenkenda and Joyce, 2014), plantations (Peerbhay et al., 2013) and tree savannahs (Cho and Mathieu, 2012) were obtained by using Worldview-2 (WV-2) data. Despite its performing technology, this sensor has not been often employed to realise vegetation analyses in African ecosystems, even though certain work related to southern African regions has been reported. For instance, in the context of South Africa, Cho and Mathieu (2012) classified five savannah species in the Kruger with an overall accuracy of 77 %, and Peerbhay et al. (2013) classified the six main tree species in KwaZulu-Natal with an overall accuracy of 85.4 %. Moreover, Karlson and Ostwald (2016) identified the five most frequently occurring tree species in an agroforestry park

in Burkina Faso, with an overall accuracy of 83.4 %. Using Quickbird images, Adelabu and Dube (2015) reported an overall accuracy of 88.8 % in the classification of five tree species.

In addition, Soti et al. (2018) highlighted the limitations of the *Pléiades* sensor in identifying tree species in a *Faidherbia Albida* agroforestry park near the Bambey city in the Old Peanut Basin of Senegal, which exhibited a global accuracy of only 38 %, requiring the authors to group the 16 targeted tree species in a single class named "tree vegetation". These results indicate that *Pléiades* data are insufficient to discriminate the tree species in the study area.

Thus, in this study, we aimed at evaluating the potential of WorldView-3 (WV-3) imagery, which involves 8 spectral bands and a spatial resolution of 1.20 m, for mapping tree diversity in a sudano-sahelian agroforestry area. To reach it, we first describe the pre-processing applied to derive the top-of-canopy reflectance data and elaborate upon a relevant technique to delimit the tree crowns and extract the representative attributes of the individual trees. Then, we describe the approaches used to analyse the spectral and textural characteristics of each tree species and identify certain tree classes by using the ground-truth data. Finally, the classification processing is described, including the technique to select the optimal classifier to discriminate the different tree species and the obtained mapping products. Subsequently, the results and their significance in the field of landscape ecology are discussed

2. Data

2.1. Study site

The study was performed in an area of 247 km^2, i.e. 13 km (16.648 °W-16.526 °W) by 19 km (14.644 °N-14.818 °N), centred on the village of Dangalma in the Bambey Department, Diourbel Region of Senegal (Fig. 1). The climate in this region is semi-arid with a short rainy season from July to October and a mean annual rainfall of 400–600 mm (Badiane et al., 2000). Human density is quite high (222 inhabitants per square kilometre), but settings are widely scattered, including 326 villages: 72 % of which having less than 500 inhabitants, 20 % having 500–1000 inhabitants, and 8% having 1000–3000 inhabitants (ANSD, 2017). 90 % of the area is under agriculture, mainly in agroforestry system (DAPSA, 2014).

The *Faidherbia albida* parkland is primarily composed of centenarian trees belonging to 27 species, that are mostly isolated and regularly distributed, with densities of only 5–9 trees/ha and even less than 4 trees/ha for 46 % and 36 % of the territory, respectively. However, this density varies considerably, increasing from the South-West to the North-East, with 15 % and 3% of the study area exhibiting a density of 10–14 trees/ha and 15–26 trees/ha, respectively. The trees are essentially associated with the pearl millet (60 % of the cropped areas) and peanut crops (28 % of the cropped areas), which are cultivated via soft practices by smallholders. Indeed, parcel size is generally less than 0.25 ha, and 69 % of the farms cover less than 3 ha. (DAPSA, 2014). Mechanisation and chemical manures are not applied, and tree and biodiversity conservation are focused on to realise pest management, soil fertilisation preservation and erosion limitation, and other ecosystem services.

2.2. Field data

We performed field surveys in the study area once a year between 2013 and 2018 to collect information regarding the trees. These surveys were scheduled at the beginning of the dry season (November/December) when the trees are leafy and crops have been harvested. The sampling sites homogeneously covered the entire study area, constituting a training database of a total of 4869 documented trees (Fig. 1-b). For each site, the species and vegetation cover rate were identified and integrated into a geographic information system (GIS) database by using the GPS recording of the geographical coordinates of these sites. Among the 27 species identified in the field, *Faidherbia albida, Balanites aegyptiaca,* and *Adansonia digitata* represented 89.5 % of the samples; the proportion of *Tamarindus indica, Anogeissus leiocarpus, Azadirachta indica,* and *Celtis integrifolia* was only 5.6 %, and the proportion of 20 rarer species was 4.9 %. Thus, we focused in this study only on the discrimination potential of the 7 most frequent species.

2.3. Remote sensing image

A cloudless Worldview-3 image (WV-3, DigitalGlobe, Inc.) covering our study area was acquired on 4 December 2017 (Fig. 1-b). At this date, most trees are still leafy and thus easily visible in images owing to the large contrast with the surrounding bare soil. The WV-3 data corresponded to a panchromatic image acquired at a spatial resolution of 0.30 m bundled with a multispectral image acquired at a spatial resolution of 1.20 m in the following 8 spectral bands: coastal blue (427 nm), blue (482 nm), green (547 nm), yellow (604 nm), red (660 nm), red-edge (723 nm), near-infrared 1 (824 nm), and near-infrared 2 (914 nm).

3. Method

3.1. Data pre-processing

The WV-3 data were delivered at the 2A-level. Therefore, we performed a radiometric calibration, followed by an orthorectification, using the ENVI 5.5 software. First, we converted the digital numbers into the absolute radiance by using the gain and offset of each spectral band. Next, we converted the absolute radiance into the top of atmosphere reflectance (TOAR), based on the sensor specifications, acquisition time and satellite attitude to determine the illumination conditions (Schowengerdt, 2007). Finally, we orthorectified the data to recover the correct geometry while discarding the topographical effects by using the metadata-file and SRTM digital terrain model with a resolution of 30 m (https://earthexplorer.usgs.gov/).

In addition, the multispectral image was merged with the panchromatic image by using the Gramm–Schmidt method via the ENVI 5.5 software to derive a multispectral pansharpened image at a resolution of 0.30 m.

3.2. Tree crown delineation

As indicated by Jakubowski et al. (2013), the delineation of trees via remote sensing is still challenging and conditions the radiometric analysis required from the basis. Although several methods with varying degrees of efficiencies have been proposed, their performance is limited owing to the low contrast between the tree canopies and their neighbourhood. In the studied image, a deep contrast exists between the trees and their background (mostly bare soil), and the individual trees are clearly isolated. Thus, the tree crowns can be extracted by simply applying a threshold on the NDVI derived from the pansharpened image. Several tests were performed to determine the optimal value for this threshold, and the value of 0.4 was noted to provide a balance between the lowest number of missing trees and the inclusion of non-tree surfaces. Next, we applied a median kernel filter of 3 pixels to regularise the thresholding, followed by the application of an opening morphological filter to separate the joint polygons. Finally, the resulting mask was vectorised and filtered to discard the non-pseudo-circle objects having a compactness index less than 1.68. In addition, we observed that most of the small selected areas were not trees, and thus, ensuring a suitable balance between false-detection elimination and number of missing small trees, we removed the objects having an area smaller than 14 m^2. In this manner, we were required to analyse only the trees with a diameter of less than 2 m, while ensuring that the mapped objects were actually trees. Finally, 134,715 isolated tree

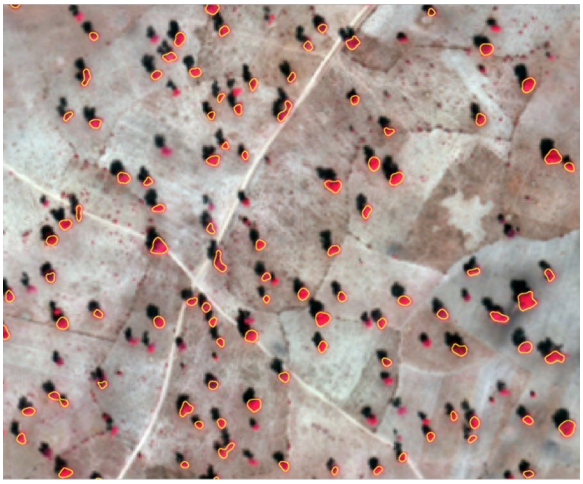

Fig. 2. Subset of the Worldview-3 image showing the delineation of tree crowns.

crowns were delineated (Fig. 2). To estimate the quality of this delineation, we randomly selected 50 test areas of 1 ha on the image, counted the number of trees correctly delineated in each area, and objects that were not trees to determine the percentage of trees that were correctly identified.

3.3. Spectral and textural analysis

The delineated tree crowns and ground-truth points (GPS) were combined to identify their intersections, and 1138 objects (0.87 % of all the delineated trees in the image) were selected as the field reference. Among these objects, 1097 belonged to the five major species and only 41 belonged to the minor species (See Table 1), reflecting their actual proportion in the study area, even though the technical limit of detecting trees with a diameter less than 2 m likely eliminated several trees belonging to the minor species.

Table 1
Number of ground-truth samples and their distribution according to the seven species.

Species	Number of samples
Faidherbia albida	823
Balanites aegyptiaca	131
Adansonia digitata (baobab)	41
Tamarindus indica	29
Azadirachta indica (neem)	32
Celtic integrifolia	23
Anogeissus leiocarpus	18
Minor species	41
Total	1138

Subsequently, we considered that the reflectance average and standard deviation of a given delineated tree crown in the 8 WV-3 spectral bands of all the pixels provide a representative signature of that tree. Fig. 3 shows the mean signature of the seven considered tree species.

The different tree species exhibited nearly similar signatures in the visible domain, except *Faidherbia albida* and *Tamarindus indica*, which exhibited slight deviations in the green (547 nm) and yellow (604 nm) bands. In the red-edge (723 nm) and infrared domain (824 nm and 914 nm), *Adansonia digitata, Anogeissus leiocarpus*, and *Celtic integrifolia* displayed a similar signature, and thus, they could not be differentiated from each other, although they were collectively clearly different from the four other species. *Faidherbia albida*, *Tamarindus indica*, *Azadirachta*

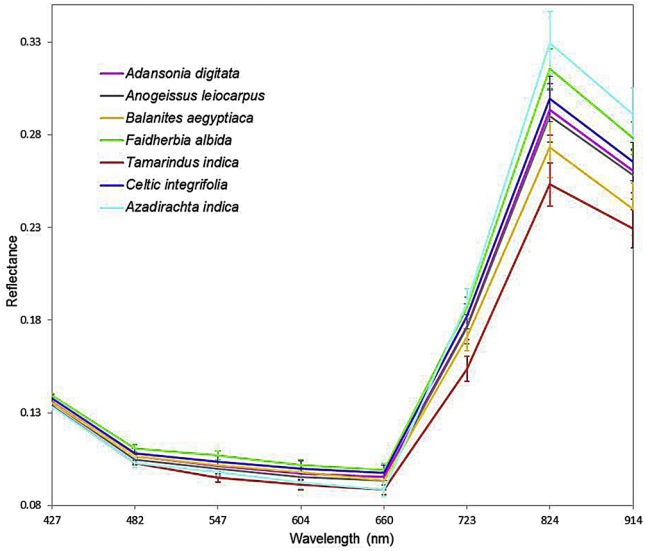

Fig. 3. Mean spectral signatures of the seven major species based on the field samples.

indica and *Balanites aegyptiaca* exhibited considerably different signatures; however, the dispersion of the radiometric values inside a given species was extremely large, and thus, the typical spectral envelopes of the species overlapped. This finding indicates that the accurate discrimination among these species may be challenging when using basic classification algorithms.

Thus, a factorial discriminant analysis (FDA) was performed on the radiometric means and standard deviations of the sampled tree population in the whole, to enhance the discrimination potential of the WV-3 spectral signature. Owing to the projection of the trees in this statistical space, the intra-class variability decreased, and the inter-class variability was enhanced; consequently, the trees could be grouped considering the common spectral trends. Therefore, it was confirmed that the trees could be clustered and the relevant classes could be selected based on the radiometric means and standard deviation data. This FDA indicated that 96 % of the total inertia of the data was included in the first three components. Fig. 4 shows the projection of the tree signatures in the three first planes defined by three first axes.

Azadirachta indica trees could be clearly distinguished from the other species on the second axis, while *Balanites aegyptiaca* and *Tamarindus indica* trees dissociated themselves from the other species on the third axis. So, they can be considered as fully separable radiometric classes. *Faidherbia albida* trees were clustered and clearly distinct from the aforementioned three species; however, they were not distinct from the minor species, namely, *Adansonia digitata*, *Anogeissus leiocarpus* and *Celtic integrifolia*. These minor species were mixed and highly scattered in the considered space and thus could not be distinguished among one another. Thus, these trees were isolated in a single class, although they could be misidentified with *Faidherbia* in some cases.

Nevertheless, we maintained *Faidherbia* as a different class because it exhibits certain characteristics in the reflectance spectra that can allow its discrimination from the trees of the three minor species. Overall, only 4 classes corresponding to the major species (*Faidherbia albida*, *Tamarindus indica*, *Azadirachta indica* and *Balanites aegyptiaca)* could be discriminated based on their spectral signature, and all the other species were grouped in a single class (other species).

In addition, we analysed the gain defined using the radiometric indices in the forms (b2-b1)/(b2 + b1) and 1.5*(b2-b1)/(b2 + b1 + 0.5) (corresponding to the NDVI and SAVI types, respectively) by combining any pair of two spectral bands out of the height available and performed a FDA on the resulting means and standard deviations of the sampled tree population. Results similar to those of the analysis of the

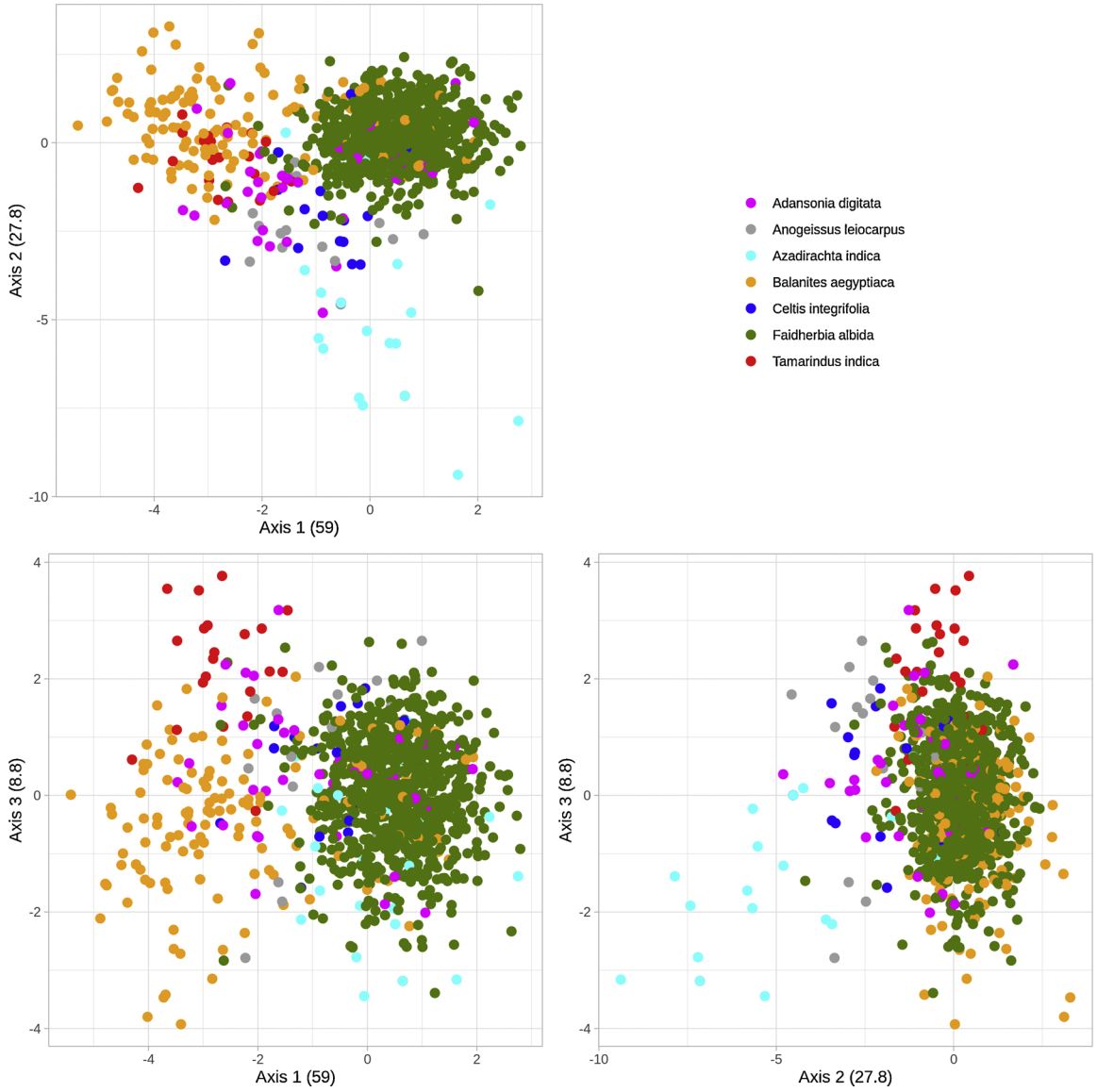

Fig. 4. Representation of factorial discriminant analysis clusters to select the distinct classes among the population of the field sampled trees.

reflectance data were obtained without any additional information. Therefore, we discarded this set of indices and focused only on the reflectance data.

Moreover, we considered the texture information that described the micro-rugosity of the tree crown image. We computed the four most diverse textural indices derived for the co-occurrence matrix: entropy, contrast, correlation and homogeneity (Haralick et al., 1973) on a sliding window of 3 × 3 pixels to describe the finest spatial variability. Each index was derived with respect to three orientations, namely, 0°, 45° and 90°, and for the four spectral bands that exhibited the largest tonal variability, that is, panchromatic, green, red, and near-infrared. None of the numerous indices indicated any variation among the individual trees of one species or those of different species. Thus, it was considered that the texture is not a suitable indicator for the trees, and we performed the subsequent analyses using only the radiometric information.

3.4. Tree species classification

The trees were classified using the R software, using the tree reflectance mean and standard deviation in the height spectral bands as the descriptive data. A supervised approach was employed, based on the following five classes: *'Faidherbia albida', 'Azadirachta indica', 'Balanites aegyptiaca', 'Tamarindus indica',* and *'other species'* regrouping the 23 remaining ones, and the system learned from a random set involving 70 % of the trees from the 1138 ground-truth trees.

We performed successive and independent random draws among the ground-truth data base by using the R software to build 30 different sets of 800 training trees (70 % of the trees in each class) and 338 validation trees (remaining 30 %), which constituted the test data for the comparison of the classifiers.

We selected two algorithms that could handle samples with a large number of variables while minimising the error during the classification process: the random forest (RF) and support vector machine (SVM) algorithms.

RF is a classification and regression algorithm that performs learning considering multiple decision trees from a random selection without repeating the training at each decision tree level (Breiman, 2001; Fawagreh et al., 2014). Two-thirds of the samples are used to train the decision trees while the remaining one-third are used in an internal cross-validation to estimate the performance of the resulting RF model (Belgiu and Drăgut, 2016; Breiman, 2001). The RF algorithms

Table 2
Global accuracy and kappa indices obtained using the random forest (RF), support vector machine with radial kernel (SVM-R), and support vector machine with linear kernel (SVM-L), applied to 30 random draws of training/validation pairs.

#sample		1	2	3	4	5	6	7	8	9	10
Global accuracy (%)	RF	81	82	84	80	82	82	83	81	84	81
	SVM-R	85	85	87	86	86	86	85	84	84	86
	SVM-L	86	86	87	85	87	87	86	86	88	86
Kappa	RF	0.54	0.55	0.6	0.51	0.53	0.53	0.55	0.51	0.61	0.51
	SVM-R	0.62	0.6	0.67	0.64	0.63	0.64	0.61	0.58	0.60	0.62
	SVM-L	0.65	0.66	0.70	0.62	0.68	0.65	0.64	0.63	0.71	0.64
#sample		11	12	13	14	15	16	17	18	19	20
Global accuracy (%)	RF	81	81	82	83	82	82	82	83	80	83
	SVM-R	85	84	85	82	85	85	86	86	85	86
	SVM-L	87	85	86	83	86	85	86	88	86	86
Kappa	RF	0.53	0.50	0.55	0.54	0.56	0.53	0.53	0.58	0.49	0.55
	SVM-R	0.61	0.57	0.62	0.53	0.63	0.61	0.65	0.66	0.60	0.64
	SVM-L	0.66	0.61	0.64	0.56	0.66	0.62	0.65	0.71	0.63	0.66
#samples		21	22	23	24	25	26	27	28	29	30
Global accuracy (%)	RF	82	82	80	83	82	83	80	81	83	82
	SVM-R	85	83	83	85	85	85	86	85	84	86
	SVM-L	86	84	86	86	87	87	87	86	86	86
Kappa	RF	0.52	0.52	0.48	0.54	0.51	0.58	0.49	0.52	0.58	0.54
	SVM-R	0.60	0.55	0.56	0.60	0.60	0.61	0.64	0.63	0.60	0.62
	SVM-L	0.65	0.59	0.63	0.62	0.66	0.68	0.67	0.65	0.64	0.64

are parameterised by the numbers of decision trees and the selected variables at each decision tree. In the considered dataset, the highest performance corresponded to 500 decision trees with 16 variables (i.e., all the variables) at each decision tree.

The SVM includes sets of related supervised learning methods that are used for discrimination (Jakkula, 2006; Vapnik, 2000). This algorithm can be used to classify 2 categories of points by assigning each point to one of the separate sub-spaces by using a hyperplane that maximises the margin and minimises a quantity proportional to the number of misclassification errors (Osuna et al., 1997). SVM algorithms are differentiated by the types of kernels, which are mathematical functions used in training processes; kernels can be linear, polynomial, Gaussian (radial basis function), or sigmoid functions (Hsu et al., 2016). In this study, we analysed the linear (SVM-L) and radial (SVM-R) functions, parameterised by the cost and the gamma values, and evaluated the performance considering cost = 1 and gamma = 0.01.

Subsequently, we tested each classification algorithm over the thirty different pairs of training/validation datasets to evaluate the robustness and stability of the classifiers. Finally, the most robust and stable classifier was selected to classify all the trees.

4. Results and discussion

4.1. Delineation of trees and extraction of sampling data

The evaluation of the crown delineation derived from the NDVI thresholding and filtering indicated that no false tree detection occurred owing to the strong criteria used to evaluate the spectral discrimination capabilities of the data. However, a loss of 29 % occurred for the trees over the whole study site: All the trees smaller than 2 m and, in rare cases, larger trees that have shed part of their foliage or have a compact shape may be discarded, and the final mapping may be incomplete. However, the mapping is robust and should be complemented with further analyses to map the small trees.

In addition, *Adansonia digitata* trees, commonly known as baobabs, are often missed under these conditions, mainly due to their irregular shape. Baobabs shed their leaves during the dry season, which leads to the observed leaf density heterogeneity and makes their isolation difficult. This aspect is a major limitation because this species provides multiple eco-services to the rural population (fruits, seeds, leaves, roots, etc.) and the environment (natural soil nutriment, biodiversity, etc.) (Kaboré and Lingani, 2011).

Moreover, the radiometric signature of *Adansonia digitata* is not typical and cannot be discriminated from that of other minor species. To improve the classification of baobabs, two strategies can be employed: 1) Acquiring a satellite WV-3 image at the end of the rainy season in mid-September, when Baobabs are fully leafy. However, at this time, other misdetections may occur as the entire vegetation cover is relatively green. 2) Using photointerpretation to identify this species, because it exhibits a characteristic shape and typical shadow. It could be also driven by specific pattern recognition software to detect and correctly delineate the trees.

The intersection between the delineated crown and ground-truth data is used to extract 1138 reference trees (cf. Table 1). This sampling is highly heterogeneously distributed, with an extremely large number of trees belonging to the *Faidherbia albida* (823) and *Balanites aegyptiaca* (131) species and extremely few trees belonging to the other species (18–41 only). Although this distribution reflects the actual proportions encountered in the fields in this area, the discrimination and classification processes might be embedded. After separating the ground-truth data into training and validation datasets, several trees remain that might be insignificant for the classification evaluation (e.g., 8 for *T. indica* and 9 for *A. indica*). Thus, the results for these classes must be analysed with caution. Nevertheless, this sampling cannot be further enhanced because *T. indica* trees are rarely present in the considered area, and *A. indica* are found mostly grouped inside villages rather than being isolated in the savannah.

The radiometric signature characterising a tree was defined using the reflectance average of all the pixels comprised inside the tree crown along with its standard deviation. It may be interesting to analyse the gain defined using other descriptors of the tree crown. However, the median, for instance, did not lead to an enhanced separability of the species signatures, and a linear SVM applied on the median and its standard deviation exhibited similar performances in terms of the global accuracy and kappa index compared with those of the mean. More complex aggregation variables may be considered if efforts are to be directed in this domain.

4.2. Assessment of classification algorithms

The results for the global accuracy and kappa index for the thirty classification tests performed using RF, SVM-R, and SVM-L are presented in Table 2. The three algorithms exhibited similar performances (80–83 % for RF, 82–87 % for SVM-R, and 83–88 % for SVM-L).

Table 3
Confusion matrix of the linear support vector machine classification having a global accuracy of 88 % and kappa index of 0.71.

Reference data							
Classified as	F.albida	B. aegyptiaca	T. indica	A. indica	Other species	Total	User's acc.
F.albida	241	11	2	3	11	268	90 %
B. aegyptiaca	2	25	2	0	1	30	83 %
T. indica	2	2	3	0	5	12	25%
A. indica	0	1	0	6	1	8	75 %
Other species	1	0	1	0	18	20	90 %
Total	246	39	8	9	36	338	
Prod. acc.	98 %	64 %	38 %	67 %	50 %		

Although, RF is a less reliable algorithm with comparatively low Kappa indices (from 0.48 to 0.60). These findings are similar to those reported by studies in which SVM and RF were compared under various classification applications: In particular, SVM tends to outperform the RF for a small number and unequal distribution of the samples (e.g., Li et al., 2015; Colditz, 2015). However, RF is suitable for high-dimensional datasets (Rodriguez-Galiano and Ghimire, 2012; Colditz, 2015), in contrast to this work in which only 16 variables were considered.

Moreover, the distribution of the trees in the different classes and the intra-class accuracies were not stable during the thirty tests varying the training/validation dataset; the SVM-L was the less sensitive to the tests.

Considering these performance indicators, we selected the SVM-L algorithm with the highest kappa index (0.71) as the optimal classifier. This algorithm also corresponded to the highest global accuracy (88 %), which is a reasonably high value for remote sensing applications. The associated confusion matrix is presented in Table 3.

In addition, we tested the SVM-L algorithm on the same thirty pairs of training/validation datasets with only the four basic spectral bands (blue, green, red, and near-infrared) available on most sensors. The global accuracies ranged from 0.81 to 0.84, which are acceptable but considerably lower than the accuracies obtained using the eight bands, with very low kappa indices ranging from 0.45 to 0.55. These findings indicate that the eight bands provided by WV-3 are required to ensure the robustness of the classification. In addition, the stability of the confusion matrix was extremely low, emphasising the need for the whole set of the height spectral bands.

4.3. Tree species mapping

The confusion matrix indicates the discrimination ability of the classifier for each class independently. *Faidherbia albida* is nearly perfectly classified (98 % producer accuracy) with an extremely high reliability (90 % user accuracy), which is important because of the major impact of this species on the ecology of the parkland. *Balanites aegyptiaca* is well classified (64 % producer accuracy) with a high reliability (83 % user accuracy), although a quarter of the samples are misclassified as *Faidherbia albida. Azadirachta indica* also corresponds to a high global accuracy (67 %) but with a lower reliability (75 %), likely due to the small number of available samples. *Tamarindus indica* is considerably more misclassified (only 38 % global accuracy). However, it is quite difficult to evaluate a classification with only 8 or 9 samples. The latter two classes present highly discriminable reflectance signatures, and thus, theoretically, must be more correctly classified. This result demonstrates the relevance of ensuring a larger field database to draw effective conclusions in the evaluation stage. The trees belonging to the other species appear to be challenging to classify because one-third of the trees are recognised as *Faidherbia albida*. This aspect was predicted by the clustering of the trees of these two classes in the FDA representation. Despite the errors in classification, the high user accuracy indicates that the results are reliable, except for those of *Tamarindus indica* owing to the low number of samples.

The linear SVM classification algorithm can thus be considered sufficiently robust to be applied to the set of trees extracted from the image over the whole study area, thereby producing a map of the trees of the Bambey parkland around Dangalma (Fig. 5).

4.4. Informative resource of spatial distribution analysis for ecology

The map clearly shows that the highest concentration and diversity of trees occur around the villages (compact multicolour patches of dots, with a majority of cyan (*Azadirachta indica*) and magenta (other species), and some orange (*Balanites aegyptiaca*), confirming the results of past in-field surveys. *Balanites aegyptiaca*, known as 'desert date', is widely distributed in the dry lands of Africa and South-Asia. All parts of the tree (roots, fruit oil, wood, leaves) are traditionally used for household applications, along with the treatment of various illnesses of humans and animals (Chothani and Vaghasiya, 2011). *Azadirachta indica*, known as 'neem', is an evergreen tree from southern and south-eastern Asia, which has been introduced to West Africa in the last 20 years. This species corresponds to 7% of the trees in the developed map (Fig. 5). These trees were planted essentially in villages for fuelwood production and shade provision and to act as a natural pesticide against insects such as mosquitoes; in addition, these trees were used in agriculture for pest control (Schmutterer, 1990). Tamarind (*Tamarindus indica*), which provides a wide range of ecosystem services (Fandohan and Assogbadjo (2010) mentioned that the rural population exploits the tree for 26 different uses), is a less abundant tree (2%). The fruit (pulp) of this tree is widely used as a condiment and in beverages (Jama et al., 2008). Tamarind seeds are useful for relieving childhood malnutrition or managing diabetes (Kilungu and Njoroge, 2002). In addition, the leaves have antibiotic properties (Nordeide and Hartley, 1996).

This diversity decreases drastically outside the villages towards the savannah, and the most dominant species (75 % of the trees in the map) is *Faidherbia albida* (green dots), which is also more scattered. These trees play an important role in enriching the soil fertility and enhancing the surrounding crop yields (Umar et al., 2013). Their inverse phenology (leafy during the dry season) is also advantageous for agroforestry because the competition with other crops growing during the wet season is minimised (Roupsard and Ferhi, 2002). Moreover, these trees produce abundant fodder for livestock during the dry season. This species is therefore frequently used in the agroforestry parklands of West Africa, where it plays a key role in supporting the local economy (Pélissier, 1980).

Lower tree densities are observed along the road axis running from West to East, especially at the South edge (visible as white patches), corresponding to eroded lands. At the North-East corner of the image, the landscape is considerably different from the remaining study area, with a higher concentration of trees and a dominance of *Balanites aegyptiaca* (orange dots).

This map allows the localisation and monitoring of the dominant tree species and provides abundant information regarding the variations in the density and diversity of the individual trees all over the study site. Consequently, this map is valuable to ensure biodiversity and

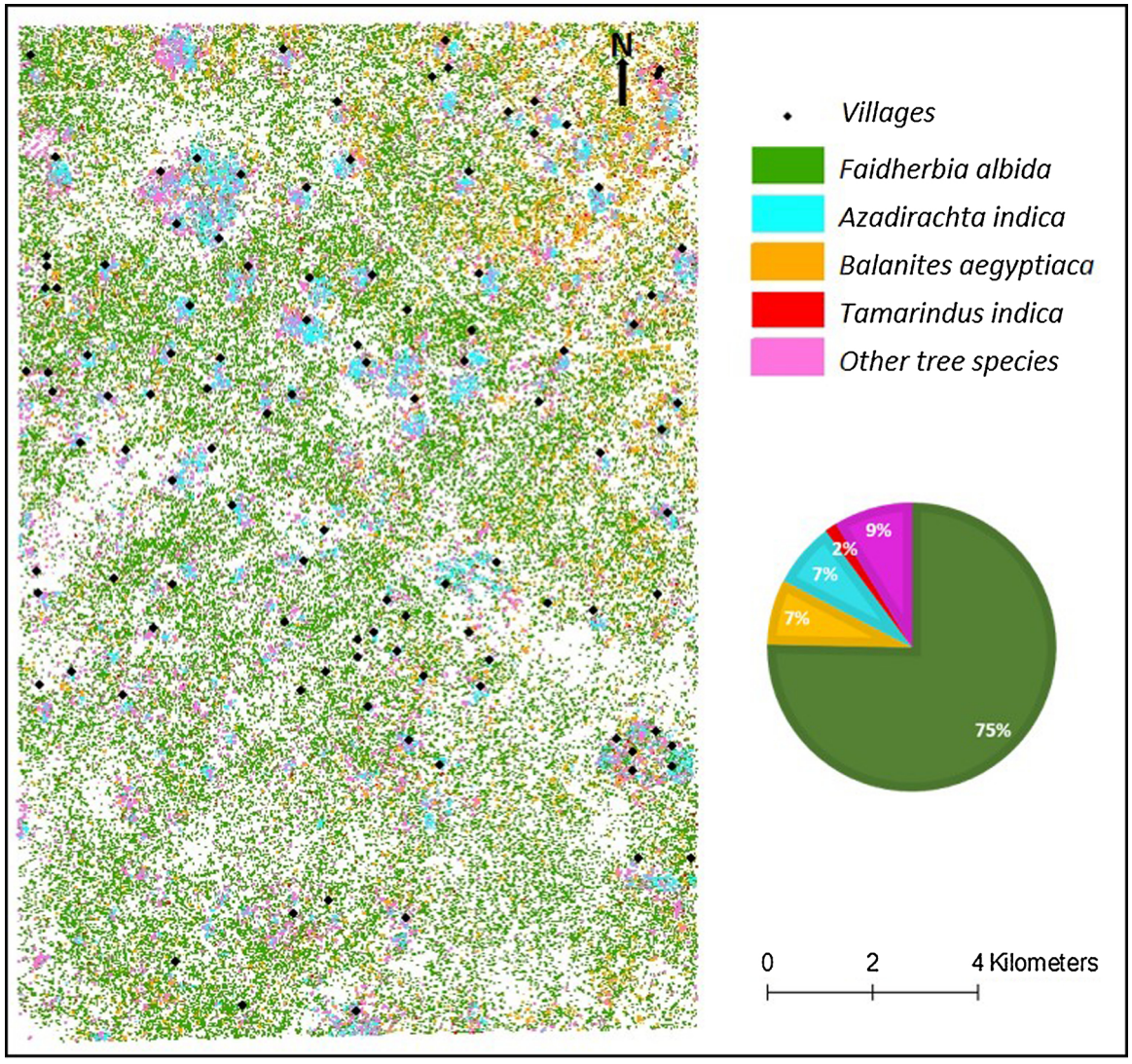

Fig. 5. Map of trees with a diameter of more than 2 m in Bambey parkland and their relative proportions.

resource management in the region. Such accurate information could help environmental protection agencies to better preserve trees and monitor the tree cover in the long term (e.g., at decadal intervals) for conservation or reforestation programmes. Trees provide a wide range of ecosystem benefits such as enhanced crop yields, provision of breeding sites for birds, biomass retention, enhanced soil fertility, and income for populations. Moreover, the presence and diversity of trees assist crop pest regulation, thereby providing an efficient agroecological alternative to chemical usage (Brévault and Clouvel, 2019). Recent studies on the Bambey *Faidherbia albida* parkland have clarified the major contribution of trees in the regulation of natural enemies and pollination of millet, which is the main food crop in the study area (Soti and Thiaw, 2019; Bagny-Beilhe and Allinne, 2019).

5. Conclusions

This work proposed a methodology to delineate individual trees and identify the major species in semi-arid parklands in Senegal, with the example of the Bambey *Faidherbia albida* parkland. Using a very high spatial resolution image acquired by WV-3 in 8 spectral bands during the dry season, we mapped all the trees with a diameter larger than 2 m. Then we classified them into four identified species, namely, *Faidherbia albida*, *Azadirachta indica*, *Balanites aegyptiaca*, and *Tamarindus indica*, which are the most abundant in this area, and a fifth class regrouping all the rarer species, including for example *Adansonia digitata, Celtic integrifolia*, *Anogeissus leiocarpus,* that could not be discriminated using the present data. The classification accuracy (88 %) is comparable to those obtained with Quickbird or WV-2 images by Adelabu and Dube (2015) or Peerbay et al. (2013) in other agroforestry parks, but much better that the results of Cho and Debba (2010) or Karlson and Ostwald (2016). Also, this classification was drastically less reliable when applied to the 4 basic spectral bands of WV-3 only, the kappa index falling from 0.71 to 0.5. Furthermore, it reaches some identification goals that were not achieved by Soti et al. (2018) with Pléiades imagery only. It shows that the choice of the appropriate imagery is still quite complex and needs further investigations. To improve the identification of the rarer species, we recommend the acquisition of a second WV-3 image at the end of the rainy season and using a combination of photo-interpretation and pattern recognition algorithms. Nevertheless, this study provides insight into the feasibility of the WV-3 images to map the trees in a Sudano-Sahelian area in Senegal, and furthermore to identify 4 of the major species, as a key element in parkland conservation and management. Overall, in the context of agroforestry systems playing a significant role in the world ecosystem, environment, economy and society, the accurate tree mapping obtained in this work could assist in conservation and management at different scales.

CRediT authorship contribution statement

Camille C.D. Lelong: Supervision, Methodology, Investigation, Formal analysis, Validation, Writing - original draft, Writing - review & editing. **Urcel Kalenga Tshingomba:** Investigation, Formal analysis, Validation, Writing - review & editing. **Valérie Soti:** Funding acquisition, Project administration, Supervision, Methodology, Writing - review & editing.

Declaration of Competing Interest

The authors declare that they have no known competing financial interests or personal relationships that could have appeared to influence the work reported in this paper.

Acknowledgements

This study was funded by the French Spatial Agency (CNES, Toulouse, France) under the TRECS project (DAR 4800000915), the CGIAR Research Programme on Grain Legumes and Dryland Cereals (GLDC-18), and CGIAR Fund Donors. We thank Ibrahima Thiaw, Babacar Ndao, Babacar Koundoul and Mor Fall who collected the field data during the project. In addition, we thank Cheikh Thiaw from the National Agronomic Research Institute (ISRA-CNRA) of Bambey and Assize Touré from the Ecological Monitoring Center (CSE) of Dakar, both of whom facilitated the landscape survey in the fields. We also acknowledge Danny Lo Seen and Annelise Tran (CIRAD, France) for reviewing the language of the manuscript.

References

Adelabu, S., Dube, T., 2015. Employing ground and satellite-based QuickBird data and random forest to discriminate five tree species in a Southern African Woodland. Geocarto Int. 30, 457–471.
Ajayi, O.C., Place, F., et al., 2011. Agricultural success from Africa: the case of fertilizer tree systems in southern Africa (Malawi, Tanzania, Mozambique, Zambia and Zimbabwe). Int. J. Agric. Sustain. 9, 129–136.
Akinnifesi, F.K., Ajayi, O., et al., 2010. Fertiliser trees for sustainable food security in the maize-based production systems of East and Southern Africa. A review. Agron. Sustain. Dev. 30, 615–629.
Alemu, M.M., 2016. Ecological benefits of trees as windbreaks and shelterbelts. Int. J. Biodivers. Sci. Ecosyst. Serv. Manag. 6, 10–13.
Alleaume, S., Dusseux, et al., 2018. A generic remote sensing approach to derive operational essential biodiversity variables (EBVs) for conservation planning. Methods Ecol. Evol. 9, 1822–1836.
ANSD, 2017. Recensement Général de la Population et de l'Habitat, de l'Agriculture et de l'Elevage (RGPHAE) 2013, Région de Diourbel, Rapport définitif, Ministère de l'Economie et des finances, Sénégal. USAID & UNFPA Ed 80p.
Badiane, A., Kouma, M., Sene, M., 2000. Région de Diourbel: gestion des eaux. In: Research, D. (Ed.), Atelier Sur Les Rapports Entre Politiques Gouvernementales Et Investissements Paysans Dans Les Régions Semi-Arides. Drylands Research, Dakar, Sénégal, pp. 18.
Bagny-Beilhe, L., Allinne, C., et al., 2019. Régulation des bioagresseurs des cultures dans les systmès agroforestiers tropicaux, revue des approches. R.
Belgiu, M., Drăgut, L., 2016. Random forest in remote sensing: a review of applications and future directions. ISPRS J. Photogramm. Remote Sens. 114, 24–31.
Bianchi, F., Booij, C., Tscharntke, T., 2006. Sustainable pest regulation in agricultural landscapes: a review on landscape composition, biodiversity and natural pest control. Proc. R. Soc. Lond., B, Biol. Sci. 273 (1595), 1715–1727.
Breiman, L., 2001. Random forests. Mach. Learn. 45, 5–32.
Brévault, T., Clouvel, P., 2019. Pest management: reconciling farming practices and natural regulations. Crop. Prot. 115, 1–6.
Cabello, J., Fernández, N., et al., 2012. The ecosystem functioning dimension in conservation: insights from remote sensing. Biodivers. Conserv. 21, 3287–3305.
Carpenter, S.R., Mooney, H.A., Agard, J., Capistrano, D., et al., 2009. Science for managing ecosystem services: beyond the millennium ecosystem assessment. Proc. Natl. Acad. Sci. 106 (5), 1305–1312.
Cho, M.A., Debba, P., et al., 2010. Improving discrimination of savanna tree species through a multiple-endmember spectral angle mapper approach: canopy-level analysis. Ieee Trans. Geosci. Remote. Sens. 48, 4133–4142.
Cho, M.A., Mathieu, R., et al., 2012. Mapping tree species composition in South African savannas using an integrated airborne spectral and LiDAR system. Remote Sens. Environ. 125, 214–226.
Chothani, D.L., Vaghasiya, H.U., 2011. A review on *Balanites* aegyptiaca Del (desert date): phytochemical constituents, traditional uses, and pharmacological activity. Pharmacogn. Rev. 5, 55–62.
Clark, M.L., Roberts, D., Clark, D., 2005. Hyperspectral discrimination of tropical rain forest tree species at leaf to crown scales. Remote Sens. Environ. 96, 375–398.
Colditz, R.R., 2015. An evaluation of different training sample allocation schemes for discrete and continuous landcover classification usin g decision tree-based algorithms. Remote Sens. (Basel) 7, 9655–9681.
Dalponte, M., Bruzzone, L., Gianelle, D., 2012. Tree species classification in the Southern Alps based on the fusion of very high geometrical resolution multispectral/hyperspectral images and LiDAR data. Remote Sens. Environ. 123, 258–270.
DAPSA, 2014. Rapport de présentation des résultats définitifs de l'enquête agricole 2013-2014. In: Ministère de l'Économie, d.F.e.d.P (Ed.), Direction de l'Analyse, de la Prévision et des Statistiques Agricoles. Dakar, Sénégal.
Dix, M.E., Johnson, R., Harrell, M.O., Case, R.M., et al., 1995. Influences of trees on abundance of natural enemies of insect pests: a review. Agrofor. Syst. 29 (3), 303–311.
Fandohan, B., Assogbadjo, A., et al., 2010. Women's traditional knowledge, use value, and the contribution of tamarind (*Tamarindus* indica L.) to rural households' cash income in Benin. Econ. Bot. 64, 248–259.
Fawagreh, K., Gaber, M., Elyan, E., 2014. Random forests: from early developments to recent advancements. Syst. Sci. Control Eng. 2.
Féret, J.-B., Asner, G.P., 2011. Spectroscopic classification of tropical forest species using radiative transfer modeling. Remote Sens. Environ. 115, 2415–2422.
Garrity, D.P., 2004. Agroforestry and the achievement of the millennium development goals. Agrofor. Syst. 61, 5–17.
Gurr, G.M., Wratten, S.D., Luna, J.M., 2003. Multi-function agricultural biodiversity: pest management and other benefits. Basic Appl. Ecol. 4 (2), 107–116.
Haralick, R.M., Shanmugam, K., Dinstein, I., 1973. Textural features for image classification. IEEE Trans. Syst. Man Cybern. 3, 610–621.
Heenkenda, M.K., Joyce, K., et al., 2014. Mangrove species identification: comparing WorldView-2 with aerial photographs. Remote Sens. (Basel) 6, 6064–6088.
Hsu, C.-W., Chang, C.-C., Lin, C.-J., 2016. A Practical Guide to Support Vector Classification. Technical report. Department of Computer Science. National Taiwain University, Taiwan, pp. 16.
Immitzer, M., Atzberger, C., Koukal, T., 2012. Tree species classification with random forest using very high spatial resolution 8-band WorldView-2 satellite data. Remote Sens. (Basel) 4, 2661–2693.
Jakkula, V., 2006. Tutorial on support vector machine (SVM). In: University, W.S. (Ed.), Ed.), School of Electronics Engineer and Computer Sciences (EECS).
Jakubowski, M., Li, W., Guo, Q., Kelly, M., 2013. Delineating individual trees from lidar data: a comparison of vector- and raster- based segmentation approaches. Remote Sens. (Basel) 5, 4163–4186.
Jama, B.A., Mohamed, A.M., Mulatya, J., Njui, A.N., 2008. Comparing the "Big five": a framework for the sustainable management of indigenous fruit trees in the drylands of East and Central Africa. Ecological Indicators. Ecological Indicators 8, 170–179.
Kaboré, D., Lingani, H., et al., 2011. A review of baobab (Adansoni digitata) products: effect of processing techniques, medicinal properties and uses. Afr. J. Food Sci. 5, 833–844.
Karlson, M., Ostwald, M., et al., 2016. Assessing the potential of multi-seasonal WorldView-2 imagery for mapping West African agroforestry tree species. Int. J. Appl. Earth Obs. Geoinf. 50, 80–88.
Kilungu, J.K., Njoroge, C.K., 2002. The compositional analysis of Adansonia digitata (baobab) and *Tamarindus* indica (tamarind) fruit seeds. Journal of Agriculture, Science and Biotechnology 4, 15–28.
Kuyah, S., Öborn, I., Jonsson, M., Dahlin, A.S., et al., 2016. Trees in agricultural landscapes enhance provision of ecosystem services in Sub-Saharan Africa. Int. J. Biodiversity Sci., Eco. Ser. Mana. 12 (4), 255–273.
Lausch, A., Bannehr, L., et al., 2016. Linking Earth Observation and taxonomic, structural and functional biodiversity: local to ecosystem perspectives. Ecol. Indic. 70, 317–339.
Li, D., Ke, Y., Gong, H., Li, X., 2015. Object-based urban tree species classification using bi-temporal WorldView-2 and WorldView-3 images. Remote Sens. (Basel) 7, 16917–16937.
Lindenmayer, D.B., Margules, C., Botkin, D., 2000. Indicators of biodiversity for ecologically sustainable forest management. Conserv. Biol. 14, 941–950.
McDermid, G.J., Hall, et al., 2009. Remote sensing and forest inventory for wildlife habitat assessment. For. Ecol. Manage. 257, 2262–2269.
Nagendra, H., 2001. Using remote sensing to assess biodiversity. Int. J. Remote Sens. 22, 2377–2400.
Nagendra, H., Munroe, D., Southworth, J., 2004. From pattern to process: landscape fragmentation and the analysis of land use/land cover change. Elsevier.
Naidoo, L., Cho, M.A., Mathieu, R., Asner, G., 2012. Classification of savanna tree species, in the Greater Kruger National Park region, by integrating hyperspectral and LiDAR data in a Random Forest data mining environment. Isprs J. Photogramm. Remote. Sens. 69, 167–179.
Nordeide, M.B., Hartley, A., et al., 1996. Nutrient composition and nutritional importance of green leaves and wild food resources in agricultural district, Koultiala, in Southern Mali. Int. J. Food Sci. Nutr. 47, 455–468.
Osuna, E., Freund, R., Girosi, F., 1997. An improved training algorithm for support vector machines. IEEE Signal Processing Society Workshop: Neural Networks for Signal Processing. IEEE, Florida, USA, pp. 276–285.
Peerbhay, K.Y., Mutanga, O., Ismail, R., 2013. Investigating the capability of few strategically placed Worldview-2 multispectral bands to discriminate forest species in KwaZulu-Natal, South Africa. Ieee J. Sel. Top. Appl. Earth Obs. Remote. Sens. 7, 307–316.
Pélissier, P., 1980. L'arbre en Afrique tropicale: la fonction et le signe. Cahiers de l'ORSTOM - Sciences Humaines 17, 127–130.
Perrings, C., Duraiappah, A., Larigauderie, A., Mooney, H., 2011. The biodiversity and ecosystem services science-policy interface. Science 331 (6021), 1139–1140.

Pettorelli, N., Bühne, H.S., et al., 2018. Satellite remote sensing of ecosystem functions: opportunities, challenges and way forward. Remote Sens. Ecol. Conserv. 4, 71–93.
Pumariño, L., Sileshi, G., Gripenberg, S., Kaartinen, R., et al., 2015. Effects of agroforestry on pest, disease and weed control: a meta-analysis. Basic Appl. Ecol. 16, 573–582.
Reid, W.V., Mooney, H.A., Cropper, A., Capistrano, D., et al., 2005. Ecosystems and human well-being Synthesis : A Report of the Millennium Ecosystem Assessment. Island Press, Washington D.C, pp. 137 2005.
Rocchini, D., Boyd, D., et al., 2016. Satellite remote sensing to monitor species diversity: potential and pitfalls. Remote Sens. Ecol. Conserv. 2, 25–36.
Rodriguez-Galiano, V.F., Ghimire, B., et al., 2012. An assessment of the effectiveness of a random forest classifier for land-cover classification. ISPRS J. Photogramm. Remote Sens. 67, 93–104.
Roupsard, O., Ferhi, A., et al., 2002. Reverse phenology and dry-season water uptake by *faidherbia albida* (del.) A. Chev. An Agroforestry Parkland of Sudanese West Africa Functional Ecology. pp. 460–472 13.
Schmutterer, H., 1990. Properties and potential of natural pesticides from the neem tree, *Azadirachta indica*. Annu. Rev. Entomol. 35, 271–297.
Schowengerdt, R.A., 2007. Remote Sensing: Models and Methods for Image Processing. Academic Press.
Sileshi, G.W., Akinnifesi, F.K., Ajayi, C., Muys, B., 2011. Integration of legume trees in maize-based cropping systems improves rain use efficiency and yield stability under rain-fed agriculture. Agric. Water Manag. 98, 1364–1372.
Soti, V., Thiaw, I., et al., 2019. Effect of landscape diversity and crop management on the control of the millet head miner, Heliocheilus albipunctella (Lepidoptera: noctuidae) by natural enemies. Biol. Control. 129, 115–122.
Soti, V., Lelong, C., Goebel, F.-R., Brévault, T., 2018. Designing a field sampling plan for landscape-pest ecological studies using VHR optical imagery. Int. J. Appl. Earth Obs. Geoinf. 72, 26–33.
Syampungani, S., Chirwa, P., Akinnifesi, F., Ajayi, O., 2010. The potential of using agroforestry as a win-win solution to climate change mitigation and adaptation and meeting food security challenges in Southern Africa. Agric. J. 5, 80–88.
Tscharntke, T., Clough, Y., et al., 2012. Global food security, biodiversity conservation and the future of agricultural intensification. Biol. Conserv. 151, 53–59.
Tscharntke, T., Karp, D.S., Chaplin-Kramer, R., Batáry, P., et al., 2016. When natural habitat fails to enhance biological pest control–Five hypotheses. Biol. Conserv. 204, 449–458.
Turner, W., Spector, S., et al., 2003. Remote sensing for biodiversity science and conservation. Trends Ecol. Evol. (Amst.) 18, 306–314.
Umar, B., Aune, J., Lungu, O., 2013. Effects of *Faidherbia albida* on the fertility of soil in smallholder conservation agriculture systems in eastern and southern Zambia. Afr. J. Agric. Res. 8, 173–183.
Vapnik, V.N., 2000. The Nature of Statistical Learning Theory. Springer-Verlag, USA.
Verchot, L., Noordwijk, M.V., et al., 2007. Climate change: linking adaptation and mitigation through agroforestry. Mitig. Adapt. Strateg. Glob. Chang. 12, 901–918.
Verlič, A., Đurić, N., et al., 2014. Tree species classification using WorldView-2 satellite images and laser scanning data in a natural urban forest. Šumarski list 138, 477–488.
Vihervaara, P., Auvinen, A.-P., et al., 2017. How essential biodiversity variables and remote sensing can help national biodiversity monitoring. Glob. Ecol. Conserv. 10, 43–59.
Waser, L., Küchler, M., Jütte, K., Stampfer, T., 2014. Evaluating the potential of WorldView-2 data to classify tree species and different levels of ash mortality. Remote Sens. (Basel) 6, 4515–4545.
World Health Organization, 2005. Ecosystems and human well-being: Health synthesis: A report of the Millennium Ecosystem Assessment 2005. World Health Organization Press, Gevena, Switzerland, pp. 53.
Wulder, M.A., Hall, R., Coops, N., Franklin, S., 2004. High spatial resolution remotely sensed data for ecosystem characterization. BioScience 54, 511–521.
Zhang, W., Ricketts, T.H., Kremen, C., Carney, K., Swinton, S.M., 2007. Ecosystem services and dis-services to agriculture. Ecol. Econ. 64 (2), 253–260.